Geophys. J. R. astr. Soc. (1984) **79**, 77–88

Geometrical theory of diffraction, evanescent waves, complex rays and Gaussian beams

L. B. Felsen *Department of Electrical Engineering and Computer Science/Microwave Research Institute, Polytechnic Institute of New York, Route 110, Farmingdale, NY 11735, USA*

Received 1984 April 27, in original form 1984 March 24

Summary. The Gaussian beam method has recently been introduced into synthetic seismology to overcome shortcomings of the ray method, especially in transition regions due to focusing or diffraction where ray theory fails. One proceeds by discretizing the initial data as a superposition of paraxial Gaussian beams, each of which is then traced through the seismic environment. Since Gaussian beam fields do not diverge in ray transition regions, they are 'uniformly regular' although the quality of this regularity depends on the beam parameters and on the 'numerical distance' which defines the extent of the transitional domain. However, when Gaussian beam patches are used to simulate non-Gaussian initial data, there arise ambiguities due to choice of patch size and location, beam width, etc., which are at the user's disposal. The effects of this arbitrariness have customarily been explored by trial and error numerical experiment but no quantitative recommendations have emerged as yet. As a step toward *a priori* predictive capability, it is proposed here to perform a systematic study on analytically tractable prototype models of how the parameters and location of a single beam affect the quality of the observed seismic field, especially in ray transition regions. The conversion of ordinary ray fields into beam fields in canonical configurations can be accomplished conveniently by displacing a real source point into a complex coordinate space. Thus, the desired beam solutions can be obtained directly from available ray, and even paraxial ray, fields. Complex ray theory and its implications are reviewed here, with an emphasis on improvements of beam tracking schemes employed at present.

1 Introduction

1.1 REAL RAYS

The ray method provides one of the important tools for predicting source excited wave motion in a complicated environment. Restricted to high frequencies, where wave propagation is a local rather than a global phenomenon, the motion is tracked in terms of local

plane waves along ray trajectories connecting the source with the observer. A *local* plane wave may be regarded as the composite wavefield that results from constructive interference of a *spectrum* of *true* plane waves; the mathematical basis for this observation is provided by stationary phase evaluation of a plane wave spatial spectral integral representation of the wavefield. The ray trajectories coincide with the direction of energy flow in the local plane wavefield, and the phase of the desired field at any point on a ray is given as the plane wave phase accumulation from the source to the observer along that ray. The amplitude of the desired field is determined from the (constant) energy contained in a narrow tube of rays surrounding the ray in question. The amplitude is inversely proportional to the square root of the energy density and hence can be ascertained from the change in ray tube cross-section between source and observer (Felsen & Marcuvitz 1973; Aki & Richards 1980).

Ray fields chart high-frequency wave transport phenomena from an initial and presumably known surface distribution to points away from the initial surface. To the lowest order of approximation, smooth variations in the medium are assumed to cause no reflections, and this requires such variations to occur over a scale length that is large compared to the local wavelength. Strong changes in the medium properties, represented by rapid variations over the scale of the local wavelength, may give rise to reflection, refraction and diffraction, as, for example, at an abrupt boundary between two different media and at a slope discontinuity in that boundary, respectively. Reflection, refraction and diffraction generate new systems of rays, excited by the incident rays. If the initial field values on each of the reflected, refracted and diffracted rays can be determined, the local plane wavefields expressed thereby can be tracked away from the initial points by the same rules as stated previously. The initial values on reflected and refracted rays at smoothly curved portions on the boundary can be established by phase and amplitude matching with the incident local plane wavefield. At scattering centres such as kinks or edges of cracks, the initial values for diffracted rays must be extracted from a high-frequency asymptotic treatment of the full 'canonical' wave solution that models the essential features of the structural discontinuity; thus, diffraction by a kink in a curved boundary can be inferred adequately from the knowledge of diffraction by the intersection of the two tangent planes, with the exterior and interior media taken globally constant at the local values near the kink in the actual environment. All of these considerations are validated to a lowest order of approximation by the above-stated requirement that smooth changes, whether in a boundary or a medium, occur over length scales that are large with respect to the local wavelength. This provides the justification for modelling direct propagation, reflection, refraction and diffraction in terms of canonical solutions with simpler local properties to furnish the various initial field values.

The preceding scenario, with varying degrees of complication that depend on the type of wavefield and the physical environment, applies in principle to all linear wave propagation and diffraction phenomena in the high-frequency limit. The method was first developed in electromagnetics under the name 'Geometrical theory of diffraction' (Keller 1965), and it has since then been refined and extended so that it is now a basic tool for analysis and for practical design in that discipline. The method has more recently been introduced into seismology (Aki & Richards 1980; Červený, Molotkov & Pšenčík 1977; Klem-Musatov & Aisenberg 1983) but refinements comparable to those in electromagnetics remain to be formulated for the considerably more complicated environmental conditions encountered there. A principal limitation of ray theory is its failure in 'transition regions' where two or more ray fields interact so strongly that the resulting rapid field variation cannot be characterized by superposition of distinct local plane waves (Felsen & Marcuvitz 1973). Such transitions occur across refraction and diffraction shadow boundaries, near

critical reflection, etc., where the number of ray species on one side differs from that on the other. Discontinuities introduced into the total ray field by the sudden disappearance or emergence of a particular ray type must be smoothed out (uniformized) by 'transition functions' based on more sophisticated wave theory. These transition functions generally contain a coordinate, configuration- and frequency-dependent parameter, the 'numerical distance' ND, whose magnitude, which is related to the difference in the phases accumulated along relevant strongly interacting rays, determines the extent of the transition region. For sufficiently large ND values, leading order asymptotics reduces a transition function to the ray field. Comparison of numerical values of the transition function and the ray field can then delineate the transitional range of ND for a specified tolerable maximum error in the ray solution.

A typical transition in a heterogeneous medium, and one that has received considerable attention in seismology, is associated with ray caustics that separate illuminated from shadow regions for a particular type of ray (Chapman 1978). Simple ray theory predicts infinite amplitudes there. Although known caustic correction factors (phase shifts) relate a ray field emerging from a caustic to its incident values before making contact, use of these corrections requires knowledge of the nature and location of the caustic. This aspect complicates numerical implementation.

1.2 COMPLEX RAYS, EVANESCENT WAVES AND GAUSSIAN BEAMS

To circumvent these difficulties, a new method (Popov 1982) has been proposed wherein the fields are transported locally not by an ordinary plane wave with constant amplitude on an equiphase surface (the wavefront) but by a beam wave whose amplitude on an equiphase surface *decays* away from the central ray, the beam axis, toward the edges of the ray tube. The amplitude profile of the paraxial beam field is expressed by a Gaussian exponential when its extent is limited to points close enough to the beam axis to validate retention of terms no higher than quadratic in the off-axis (transverse) coordinates. Within the context of the discussion above, when viewed as a spectrum of true plane waves with amplitudes determined by the Gaussian taper, the transport properties of the constructive interference maxima of this wave bundle may be described by stationary phase analysis as before, with the important difference that the stationary phase points in the spatial wavenumber spectrum are generally complex (Felsen 1975, 1976). Thus, the beam wavefield is synthesized locally by (evanescent or inhomogeneous) plane waves with complex phase, in contrast to the real phase ordinary plane waves that synthesize the conventional ray field. By direct extension of the notion of a ray as the plane wave trajectory defined by the spatial wavenumbers, one is led to the conclusion that if the spatial wavenumbers are complex, the trajectory must lie in a complex coordinate space obtained by analytic continuation of the physical coordinates from real to complex values. By extending initial conditions (Ghione, Montrosset & Felsen 1984; Einziger & Felsen 1982) and environmental parameters into the complex space, one may trace complex ray fields by the (analytically continued) rules applicable to real ray fields. Where a complex ray intersects the real coordinate space, it furnishes there an observable field. These considerations incorporate beam waves systematically within the framework of ray theory, provided that the category of real rays is enlarged to include complex rays.

An important attribute of transition phenomena associated with the complex ray fields that represent evanescent waves is that these phenomena generally occur in localized regions in the *complex* coordinate space (Ghione *et al.* 1984; Heyman & Felsen 1983). For example, a complex ray field may give rise to a complex caustic where ray tube cross-sections shrink to zero and thus invalidate complex ray theory there, but these cross-sections remain finite

at the real space intersections. If the caustic surface never intersects the real coordinate space, complex ray theory remains valid throughout while real ray theory with its real-space caustic fails in the transition region. This complex ray interpretation of the wave bundle that synthesizes a paraxial beam thus makes beam phenomena understandable as ray phenomena associated with evanescent instead of ordinary local plane waves. To repeat, ray theory comprising real and complex ray fields can account for *all* high-frequency wave phenomena, including those (for example, beam type fields and fields on the shadow side of real caustics) where evanescent fields predominate. If a complex ray transition region approaches the real coordinate space, it may be necessary to correct the affected ray fields by transition functions in order to obtain more accurate predictions, although ray field infinities do not occur. The numerical distance $\overline{ND}$, now complex, determines the extent of the transition region.

The preceding discussion clarifies the above-noted motivation for seeking to decompose a given wavefield into (local evanescent) beam waves instead of local ordinary plane waves if transition phenomena for the former, where ray theory fails, may thereby be removed from the physical space. Transitions near certain caustics generated by focusing due to medium inhomogeneities fall into this category. How deep a ray field transition region is pushed into the complex space depends on how strongly evanescent the constituent plane waves are, i.e. on the parameters of the paraxial beam. Transition regions deep within the complex space may have real-space fields that are so diffuse as to eliminate entirely the physically observable transition effects caused by non-evanescent wave constituents. To retain such details in the wave behaviour, the incident wavefield should only be weakly evanescent, but then simple ray theory without uniformizing corrections may be strained by the proximity of the transition region to real coordinate space. Effective use of the Gaussian beam method requires a balance between these conflicting attributes.

One may now understand better the dilemma posed when modelling non-evanescent initial conditions locally by evanescent conditions, as proposed in the Gaussian beam method. By properly adjusting the plane wave spectral amplitudes in the beam superposition integral that expresses the initial surface field, and performing the stationary phase evaluation that selects the constructively interfering wave groups, one may indeed compensate for the local beam character and generate off-surface fields which agree asymptotically with those predicted by conventional (non-evanescent) ray theory (Popov 1982). However, the numerical implementation of the method involves discretization of the integral into Gaussian beam patches. Since not only the location and degree of overlap of the patches but also the initial beam parameters, which determine the evanescence and hence the complexness of the ray bundle, are at the user's disposal, there exists an arbitrariness whose effects have been assessed so far only by trial and error numerical experiment and comparison with reference solutions obtained by other algorithms with proved reliability (Červený, Popov & Pšenčík 1982; Nowack & Aki 1984). Although these comparisons have granted qualitative insight into how various beam parameters affect the resulting seismogram, no quantitative recommendations have emerged from these studies. Thus, the Gaussian beam method at present lacks *a priori* predictive capability.

1.3 COMPLEX SOURCE POINTS AND GAUSSIAN BEAMS

To remedy some of these deficiencies, it would seem to be advisable to determine the influence of the beam parameters on wave phenomena associated with bulk propagation, reflection, refraction and diffraction of Gaussian beams in rigorously based *analytical* prototype models. Analytical models involving plane wave decomposition of a Gaussian

beam are inefficient here since the plane wave response cannot generally be ascertained in a fairly arbitrary environment. Even in those special cases amenable to plane wave spectral decomposition, asymptotic reduction of the spectral integral requires an additional step. These complications can be avoided by recourse to complex ray theory or, more fundamentally, to *rigorous wave theory* performed in a *complex coordinate space.*

It is remarkable, and easily proved, that by assigning a complex value $\mathbf{r}_b' = \mathbf{r}_0 + i\mathbf{b}$, where $\mathbf{r}_0$ and $\mathbf{b}$ are real vectors, to the location $\mathbf{r}'$ of a source point in a homogeneous unbounded medium, one thereby converts the time-harmonic spherically (three-dimensional) or cylindrically (two-dimensional) spreading field into a wavefield with directional properties (Deschamps 1971; Felsen 1976). By proper choice of the imaginary part $i\mathbf{b}$, the complex source point substitution generates a field whose maximum lies along the direction $\mathbf{b}_0$ of the vector $\mathbf{b}$ and whose amplitude decays exponentially away from the $\mathbf{b}_0$ direction; the rate of decay depends on the magnitude $b = |\mathbf{b}|$. Thus, the field behaves like a beam whose maximum lies along the beam axis $\mathbf{b}_0$; its narrowest portion, the beam waist, is centred at the real location $\mathbf{r}_0$. Since the source coordinate $\mathbf{r}'$ appears only as a parameter in the field equations for the Green's function $G(\mathbf{r}, \mathbf{r}')$, the beam field $G_b(\mathbf{r}, \mathbf{r}_b')$ obtained by analytic continuation to complex source location is an *exact* solution of the field equations if $G(\mathbf{r}, \mathbf{r}')$ itself is exact. In the vicinity of the $\mathbf{b}_0$-axis, a paraxial approximation of G_b furnishes precisely a paraxial Gaussian beam. This paraxial Gaussian beam field can also be found directly on replacing $\mathbf{r}'$ by $\mathbf{r}_b'$ in the paraxial ray approximation of $G(\mathbf{r}, \mathbf{r}')$. Viewed asymptotically at high frequencies, the source point in complex space emits complex rays whose real-space intersections define a beam-type field, which agrees with the conventional paraxial Gaussian beam in the vicinity of the beam axis $\mathbf{b}_0$. It should be noted that the complete complex ray field furnishes a rigorous asymptotic solution of the field equations whereas the paraxial Gaussian beam is only an approximate solution. Finally, the complex source point method can generate not only the lowest order Gaussian beam but also, by complex displacement of multipole sources, Gaussian beams of higher order (Shin & Felsen 1977). This observation may be important for seismic source models that are based on an assumed multipole behaviour.

It now follows that if the point or line source Green's function $G(\mathbf{r}, \mathbf{r}')$ is known exactly or asymptotically in a given environment, its analytically continued form $G_b(\mathbf{r}, \mathbf{r}_b')$ provides an exact or asymptotic solution for an exciting beam wave in the same environment. Thus, by the complex source point substitution, a rigorous treatment of Gaussian beams in various environments can be obtained directly from the corresponding treatment of ordinary ray fields in this environment. The beam solution so obtained is synthesized by complex ray fields, each ray being descriptive of an evanescent plane wave with fixed complex spectral wavenumbers. The local evanescent plane waves are automatically tracked in real space by evaluating $G_b(\mathbf{r}, \mathbf{r}_b')$ at different observation points $\mathbf{r}$.

Since paraxial Gaussian beam fields are analytic continuations of point or line source excited real ray fields, the behaviour of direct, reflected, refracted and diffracted beams can be ascertained from the behaviour of real ray fields on replacement of $\mathbf{r}'$ by $\mathbf{r}_b'$ in the ray phase and amplitude functions, and in the ray reflection, refraction and diffraction coefficients. Moreover, one may now clearly assess how replacement of a real ray field affects the behaviour in critical regions, the transition regions, where ray theory fails. As noted previously, the onset of failure in a given transition region can be ascertained from the 'numerical distance', ND, descriptive of the transition in question. When ND is so small that the transition function cannot be approximated satisfactorily by the leading term in its large ND asymptotic expansion, the ray theory breaks down. The 'satisfactory' range can be defined explicitly in terms of a specified maximum acceptable error by comparing the

asymptotic form of a the transition function with numerical data for its exact value. For real ray fields, the (real) numerical distance inevitably goes to zero on or near the transition boundary (caustic, shadow boundary, etc.). For complex ray (beam) fields, the complex numerical distance $\overline{ND}$ for many types of transitions does not vanish at real observation points (Felsen 1976; Green, Bertoni & Felsen 1979). Therefore, in principle, beam theory always applies. However, depending on $|\mathbf{b}|$, the $\overline{ND}$ may become so small that the Gaussian beam solution deviates markedly from the solution obtained by the transition function evaluated at these $\overline{ND}$ values. Thus, the previously imposed criterion of maximum error serves as well to establish the acceptability, or not, of the Gaussian beam field. While the Gaussian beam solution will not fail, it may be unacceptably inaccurate.

The Gaussian beam field, especially for diffraction and near critical reflection, depends not only on the width of the incident beam but also on where the beam axis is located with respect to the diffraction point or the critically incident ray. By systematic numerical comparisons between real and complex source point solutions for canonical configurations, one may establish acceptability criteria phrased in terms of the $\overline{ND}$. Since diffraction effects are exhibited most strongly when the beam axis coincides with the transitonal ray, a weak response due to a displaced incident beam might be corrected by adjusting its origin on the initial surface. Such a refined procedure could conceivably be incorporated into a numerical programme to enhance a submerged diffraction effect.

The preceding considerations are aimed at quantifying the Gaussian beam method for transition phenomena associated with real ray fields. However, complex ray theory also plays a role in the proper structuring of reflected, refracted and diffracted beam fields outside the ray transition regions. It has been proposed (Červený & Pšenčík 1984) that the reflection and transmission coefficients for a paraxial beam reflected or transmitted at an interface between two media should be taken as the Fresnel reflection and transmission coefficients for a plane wave incident along the (real) beam axis. Reduction of the complex ray solution to the paraxial region reveals, however, that the incidence angle in these formulas should not be the real ray angle of the beam axis but the complex angle that contains in it the complex displacement of the source point (Ra, Bertoni & Felsen 1973). This is due to the fact that although the beam axis is a real ray, the paraxial ray tube surrounding it comprises complex rays. For example it is this complex part of the incidence angle that incorporates into the reflected complex ray field the lateral beam shift that has been well explored in optics and acoustics. The beam modifications produced by use of the complex incidence angle in reflection and transmission coefficients can be related to the excitation of higher order beam modes that describe the deviation of the reflected or refracted beam profile from its geometrically predicted value. Thus, a reflected lowest order Gaussian beam at a shifted location, or with some asymmetry, is equivalent to a combination of higher order beams with respect to the non-shifted location. Clearly, the former representation obtained by the complex source point method is physically more incisive and numerically more efficient. Therefore, the simple inclusion of complex angles for reflection and transmission coefficients should already serve to improve results (Červený & Pšenčík 1984) computed by the Gaussian beam method. The same observations hold when ray diffraction coefficients (for example, due to a kink in a boundary) are extended to describe diffraction by a beam.

Finally, since the complex source point method generates exact beam solutions of the time-harmonic field equations, causality remains imposed when transforming these into the time domain. Here again, approximate numerical schemes for implementing beam-type solutions based on complex source points may be less apt to violate causality than those based on other beam models.

The complex source point field for the scalar wave equation and its paraxial approximation are summarized below, with observations pertaining to how this incident paraxial beam field can be employed systematically to derive reflected, refracted and diffracted fields. Specific applications to various canonical configurations are reserved for a future publication. These applications address effects of edges, corners or kinks, interfaces between different media, curved interfaces or boundaries, and refractive medium inhomogeneities.

2 The complex source point field

We shall be concerned here with solutions for the scalar time-harmonic Green's function $G(\mathbf{r}, \mathbf{r}')$ in various physical environments, when the originally real source point $\mathbf{r}'$ is assigned complex values $\mathbf{r}'_b$ but the observation point $\mathbf{r}$ is kept real. The Green's function is defined by the inhomogeneous scalar wave equation

$$(\nabla^2 + k^2)\, G(\mathbf{r}, \mathbf{r}') = -\delta(\mathbf{r}-\mathbf{r}') \tag{1}$$

subject to boundary conditions that model the physical structure. $k = \omega/v = 2\pi/\lambda$ is the wavenumber in the medium with velocity v, ω is the radian frequency, λ is the wavelength, and a time factor $\exp(-i\omega t)$ is suppressed. In a multilayer environment with velocity v_i in the ith layer, $G \to G_i$ and $k \to k_i$ in the ith layer, and the right-hand side in (1) is set equal to zero except for the layer containing the source. Continuity of G_i and its normal derivative, suitably weighted, across the layer boundaries is imposed, and if a layer extends to infinity, a radiation condition is appended. G can be regarded as a scalar potential, from which vector fields are then generated by appropriate vector differentiation.

Since $\mathbf{r}'$ appears as a parameter in (1), the analytic continuation of $G(\mathbf{r}, \mathbf{r}')$ to $G(\mathbf{r}, \mathbf{r}'_b) = G_b(\mathbf{r}, \mathbf{r}'_b)$, when possible, continues to satisfy the wave equation *and* boundary conditions *exactly*. Here, $\mathbf{r}'_b = \mathbf{r}_0 + i\mathbf{b}$, is complex, with $\mathbf{r}_0$, $\mathbf{b}$ real. The source term is now no longer a delta function but the *equivalent source distribution* in real space can be inferred from $G_b(\mathbf{r}, \mathbf{r}'_b)$ by examining the behaviour of that function as $\mathbf{r} \to \mathbf{r}_0$.

2.1 FREE SPACE – THE INCIDENT FIELD

In an unbounded homogeneous medium, the Green's function is given by

$$G(\mathbf{r}, \mathbf{r}') = \frac{\exp(ikD)}{4\pi D}, \quad D = \sqrt{(x-x')^2 + (y-y')^2 + (z-z')^2} \tag{2}$$

in three dimensions, and by

$$\bar{G}(\bar{r}, \bar{r}') = \frac{i}{4} H_0^{(1)}(k\bar{D}), \quad \bar{D} = \sqrt{(y-y')^2 + (z-z')^2} \tag{3}$$

in two dimensions (y, z). Here, (x, y, z) denote rectangular coordinates. To satisfy the radiation condition, the distances D and $\bar{D}$ from the source to the observer are taken to be positive real.

When $\mathbf{r}' \to \mathbf{r}'_b = \mathbf{r}_0 + i\mathbf{b}$, i.e.

$$x' \to x_0 + ib_x, \; y' \to y_0 + ib_y, \; z' \to z_0 + ib \tag{4}$$

the distances $D \to D_b$ and $\bar{D} \to \bar{D}_b$ become complex. To continue to satisfy the radiation condition, and to reduce G_b and $\bar{G}_b$ to G and $\bar{G}$, respectively, when $|\mathbf{b}| \to 0$, one imposes on the complex distances the condition (Fig. 1a)

$$\mathrm{Re}\, D_b > 0, \; \mathrm{Re}\, \bar{D}_b > 0. \tag{5}$$

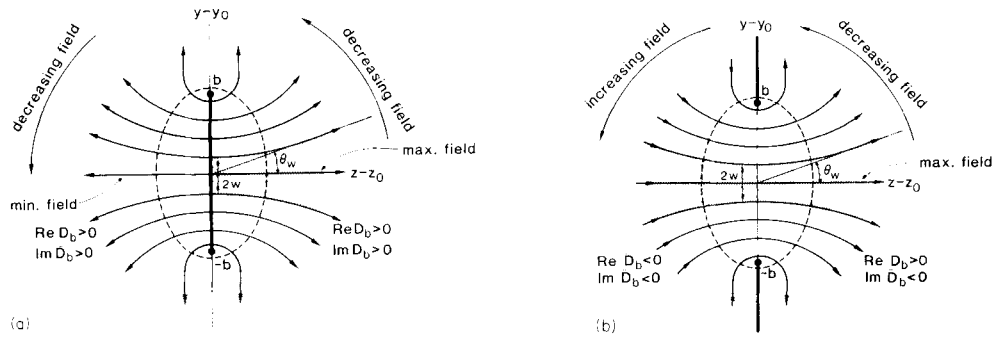

Figure 1. Phase paths on which $\mathrm{Im}\,\bar{D}_b$ = constant (solid) and phase fronts on which $\mathrm{Re}\,\bar{D}_b$ = constant (dashed) for alternative definitions of the top Riemann sheet of $\bar{D}_b$. Branch cuts are drawn heavy. Arrows denote the direction of propagation of the phase front. Conditions are symmetrical with respect to the $(z - z_0)$-axis. Paraxial beam region shown shaded. $2W = 2\sqrt{2b/k}$ is the (1/e) beam width at the waist. $2\theta_w = 2\sqrt{2/kb}$ is the angular beam width in the far zone. (a) $\mathrm{Re}\,\bar{D}_b > 0$ on top sheet. Branch cut along $\mathrm{Re}\,\bar{D}_b = 0$. (b) $\mathrm{Im}\,\bar{D}_b < 0$ on top sheet. Branch cuts along $\mathrm{Im}\,\bar{D}_b = 0$.

D_b and $\bar{D}_b$ represent, respectively, the complex radii of curvature of the phase fronts descriptive of the outgoing 3-D and 2-D complex ray field. For the 2-D field, the complex observation angle $\bar{\theta}_b$ is defined as

$$\bar{\theta}_b = \tan^{-1}\left(\frac{y - y_0 - ib_y}{z - z_0 \quad ib_z}\right) = \sin^{-1}\left(\frac{y - y_0 - ib_y}{\bar{D}_b}\right) \tag{6}$$

and similar definitions identify angular coordinates in the 3-D complex space.

To understand the implications of (4), consider the special case $b_{x,y} = 0$, $b_z = b$. Then in the plane $z = z_0$, $\mathrm{Re}\,D_b = 0$ and $\mathrm{Re}\,\bar{D}_b = 0$ for $D_t^2 \equiv (x - x_0)^2 + (y - y_0)^2 < b^2$ and $(y - y_0)^2 < b^2$, respectively. Branch cuts may be chosen along the contours $\mathrm{Re}\,D_b = 0$ and $\mathrm{Re}\,\bar{D}_b = 0$, which connect the branch points at $D_t = \pm b$ and $(y - y_0) = \pm b$, respectively. Then if $\mathrm{Re}\,D_b$ and $\mathrm{Re}\,\bar{D}_b$ are defined to be positive away from the cut, these quantities will be positive everywhere on the top sheet of the Riemann surface defined in this manner. With this definition, D_b or $\bar{D}_b$ equals $(z - ib)$ along the positive z-axis but $(-z + ib)$ along the negative z-axis, yielding for G_b the corresponding exponential field strengths $\exp(kb)$ and $\exp(-kb)$, respectively. Analogous remarks apply to $\bar{G}_b$. The choice $b > 0$ therefore generates wavefields that have an exponential maximum along the positive z-axis and an exponential minimum along the negative z-axis (Fig. 1a). Such fields have a beam-like character in the half-space $z > 0$. The regions $D_t < |b|$ and $|y - y_0| < |b|$ may be regarded as equivalent circular and linear source regions which generate the initial distribution for the 3-D and 2-D fields G_b and $\bar{G}_b$, respectively (Fig. 1a). For the 3-D case, the initial distribution is

$$G_b\Big|_{z=z_0} = \frac{i\exp[(k\sqrt{b^2 - D_t^2})]}{4\pi\sqrt{b^2 - D_t^2}}, \qquad D_t < b,\ b > 0 \tag{7a}$$

$$= \frac{\exp[(ik\sqrt{D_t^2 - b^2})]}{4\pi\sqrt{D_t^2 - b^2}}, \qquad D_t > b \tag{7b}$$

with all square roots defined to be positive. Thus, the equivalent sources in real space generate an initial equiphase aperture distribution that is exponentially tapered away from

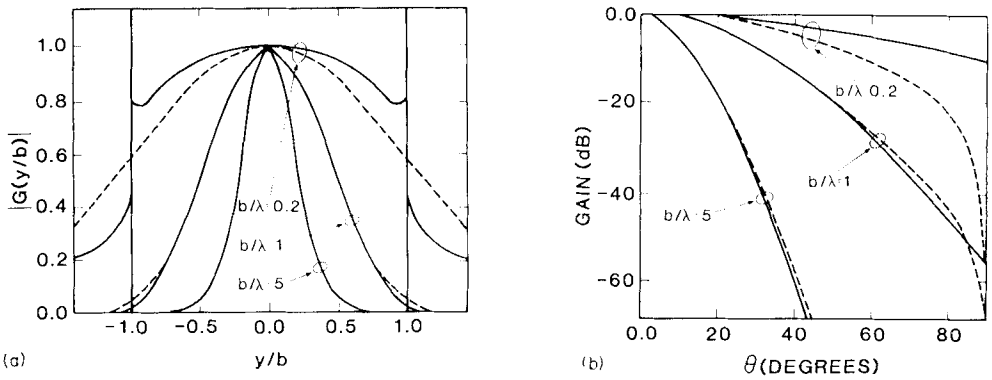

Figure 2. Comparison of complex source point field and field due to infinite aperture distribution with Gaussian profile $\exp[-k(y-y_0)^2/2b]$, for various b/λ (2-D). Solid curves: complex source point field. Dashed curve: Gaussian aperture profile. The complex source point field is seen to simulate the effects of a Gaussian aperture field very well for $b/\lambda \geqslant 1$. (a) Aperture field. The complex source point field has an algebraic singularity at $|y - y_0|/b = 1$, which cannot be resolved here for $b/\lambda \geqslant 1$. (b) Far zone field.

the aperture centre but peaks algebraically near the aperture edge at $D_t = b$. The peaking is weaker than the $(1/D_t)$ behaviour corresponding to a real point source ($b = 0$), owing to the fact that displacement of the source into the complex coordinate space smears out its effect in real space. Unless kb is very small, the effect of this peaking near $D_t = b$ is negligible when considering the aperture field as a whole, which has a maximum amplitude $\exp(kb)/4\pi b$ at the aperture centre. Outside the source region ($D_t > b$), the field in the aperture plane behaves like an outgoing wave. Analogous remarks apply to $\bar{G}_b$ (see Fig. 2a).

One may readily establish that the surfaces of constant exponential amplitude (Im D_b = constant) and constant phase (Re D_b = constant) form, respectively, a family of confocal hyperboloids and ellipsoids, with focus at $D_t = b$. Thus, the region of greatest concentration of the field (the waist of the beam) lies on the $z = 0$ plane. The hyperboloids define the 'phase paths' of the local evanescent plane waves that carry the field from the aperture into the far zone. The degree of evanescence of these local plane waves becomes weaker with distance from the aperture, and it tends to zero in the far zone where the phase paths degenerate into radial trajectories (the conical asymptotes of the hyperboloids) which coincide with the conventional real ray paths for non-evanescent local plane waves. Within the framework of complex ray theory, the phase paths track the real-space intersections of those straight-line complex rays from the complex source point that generate on each such path a field with constant exponential amplitude. In the far zone, where $D^2 = D_t^2 + z^2 \gg b^2$, one has

$$D_b \sim D - ib\cos\theta, \qquad \cos\theta = z/D \tag{8}$$

so that the far field

$$G_b \sim \frac{\exp(ikD)}{4\pi D}\exp(kb\cos\theta) \tag{9}$$

exhibits a pattern function $f(\theta) = \exp(kb\cos\theta)$ descriptive of a beam with maximum along the z-axis. While the field is defined in the entire physical space $0 < \theta < \pi$ (see Fig. 1a), it simulates a conventional beam field only in the half-space $0 < \theta < \pi/2$. A distant observer in the aperture plane $\theta = \pi/2$ sees a field amplitude diminished by a factor $\exp(-kb)$ from the maximum on the beam axis. Analogous conclusions for the 2-D field follow from the

asymptotic approximation

$$\bar{G}_b \sim \frac{1}{4}\sqrt{\frac{2}{\pi k \bar{D}_b}} \exp(ik\bar{D}_b + i\pi/4), \qquad k\,|\,\bar{D}_b\,| \gg 1 \tag{10}$$

which may be employed at all observation points except those near the edges of the equivalent aperture.

Near the beam axis, the ellipsoidal equiphase surfaces can be approximated by spheres. The region of validity of this approximation is the paraxial region wherein $D_t^2 \ll (z^2 + b^2)$ so that

$$D_b \sim z - ib + \frac{D_t^2}{2(z - ib)} = z - ib + \frac{zD_t^2}{2(z^2 + b^2)} + \frac{ibD_t^2}{2(z^2 + b^2)} \tag{11}$$

$$= D_{b0} + (\partial D_b/\partial D_t)_0 D_t + (\partial^2 D_b/\partial D_t^2)_0 D_t^2/2 + \ldots \tag{11a}$$

The subscript 'o' implies evaluation at $D_t = 0$. $D_{bo} = (z - ib)$ identifies the complex radius of curvature of the on-axis beam field. Note that although the beam axis follows the real ray trajectory $\theta_b = 0$ (*cf.* (6), with $b_{x,y} = 0$, $b_z = b$), the ray tube surrounding the axis contains complex rays. The resulting field

$$G_b \sim \frac{\exp\{ik(z - ib) + kD_t^2/2(z - ib)\}}{4\pi(z - ib)} \tag{12a}$$

$$= \frac{\exp(kb)}{4\pi(z - ib)} \exp\left[ikz\left(1 + \frac{D_t^2}{2(z^2 + b^2)}\right) - kb\frac{D_t^2}{2(z^2 + b^2)}\right] \tag{12b}$$

agrees with what is conventionally referred to as a paraxial Gaussian beam. Near and on the aperture plane, the (1/e) half-width of the paraxial beam is $W = \sqrt{2b/k}$; from (8), the corresponding hyperbolic paths emerge in the far zone with the (1/e) angular width $\theta_w = \sqrt{2/kb}$ (see Fig. 1). Evident modifications, via (9), yield the results for the 2-D case. Numerical comparison shows that the complex source point field agrees well with the field due to an infinite Gaussian aperture distribution for $b/\lambda \geq 1$ (Fig. 2).

When b_x, $b_y \neq 0$, all of the above considerations apply except that the beam axis is now rotated to lie along the vector $\mathbf{b} = (b_x, b_y, b_z)$. It should be noted in this connection that the complex source point substitution must be performed on an *arbitrarily placed* real source point $\mathbf{r}'$ in order to convert a spherical wavefield into a beam field that can be steered in any specified direction. If the beam waist is to be located on the z-axis, for example, one cannot employ $\mathbf{r}' = (0, 0, z')$ at the start since analytic continuation of the transverse source coordinates is not possible from zero initial values $x' = y' = 0$. By the correct procedure, non-vanishing source coordinates (x', y', z') are continued into the complex coordinate space and the condition $x_0 = y_0 = 0$ is imposed thereafter to place the waist of the beam on the z-axis.

The *outgoing* wave restriction in (5) everywhere on the *top* sheet of the Riemann surface for the complex distance implies that the resulting field behaves like a beam only in the region $(z - z_0) > 0$ (we assume again that $b_{x,y} = 0$). The *incoming* portion of a beam in the region $z < z_0$ requires $\mathrm{Re}\, D_b$ or $\mathrm{Re}\, \bar{D}_b < 0$, a behaviour satisfied on the *lower* Riemann sheet. The entire beam can be contained on a top sheet defined by the condition

$$\mathrm{Im}\, D_b < 0, \qquad \mathrm{Im}\, \bar{D}_b < 0 \tag{13}$$

with cuts conveniently chosen along the contours $\mathrm{Im}\, D_b = 0$ or $\mathrm{Im}\, \bar{D}_b = 0$ (Fig. 1b). However, other choices of cuts extending from the branch points to infinity are equally possible,

with a consequent more complicated partitioning of the top sheet with respect to the behaviour of the real and imaginary parts of the complex distances.

2.2 ENVIRONMENTAL EFFECTS

Having found that, for values of $b/\lambda \geqslant 1$, the complex source point field agrees very well in the near zone (Fresnel region) and the far zone with the field of an aperture distribution that extends the paraxial Gaussian profile indefinitely, one may now model the effect of an environment on an incident Gaussian beam field as the effect of that same environment on the complex source point field. The latter, in turn, may be found from the geometrical ray solution for a real source point by the complex source point substitution. One may explore in this manner the interaction with the environment of *any* portion of the Gaussian incident beam, including the weak fields far from the beam axis. Thereby, one may assess, by numerical comparisons, the dependence of an observed field response on the degree of evanescence of the local incident plane waves and define the paraxial region and the beam width parameter so that essential features of a non-Gaussian input, which is modelled by superposition of Gaussian beams, are not obliterated. In the paraxial region, expressions for relevant quantities can be obtained by paraxial expansion about their on-axis value. Although the beam axis follows a real ray trajectory, care must be taken to use the proper *complex* ray parameters in this expansion, as illustrated in (11a) for the incident free space field. For example, if $\Gamma(\bar{\theta}, \bar{\theta}')$ denotes a reflection, transmission, or diffraction coefficient that provides the initial amplitude on a reflected, transmitted or diffracted ray progressing along the observation angle $\bar{\theta}$ when a real ray field is incident along the angle $\bar{\theta}'$, then $\Gamma_b(\bar{\theta}_b, \bar{\theta}'_b)$ denotes the corresponding coefficient for the incident Gaussian beam whose axis lies along $\bar{\theta}'_b$, with the complex angles defined according to (6). The paraxial expansion about the real on-axis coefficient $\Gamma(\bar{\theta}, \bar{\theta}')$ must take the form

$$\Gamma_b(\bar{\theta}_b, \bar{\theta}'_b) = \Gamma(\bar{\theta}, \bar{\theta}') + \frac{\partial \Gamma_b}{\partial \bar{\theta}_b}\bigg|_{\bar{\theta}} (\bar{\theta}_b - \bar{\theta}) + \frac{\partial^2 \Gamma_b}{\partial \bar{\theta}_b^2}\bigg|_{\bar{\theta}} (\bar{\theta}_b - \bar{\theta})^2/2 + \ldots \tag{14a}$$

$$\equiv \Gamma(\bar{\theta}, \bar{\theta}') + \Delta\Gamma \tag{14b}$$

$$\approx \Gamma(\bar{\theta}, \bar{\theta}')\, e^{\delta}, \qquad \delta = (\Delta\Gamma)/\Gamma \ll 1. \tag{14c}$$

Thus, the real ray coefficient Γ is modified by a (generally complex) phase correction that may re-locate the maximum of the reflected, transmitted or diffracted beam field and hence the corresponding beam axis, as well as introducing asymmetries into the beam profile. This correction factor has so far been omitted from the Gaussian beam calculations reported in the seismic literature.

3 Conclusions

To sum up, the Gaussian beam method offers what seems to be an attractive option for computing seismograms in complicated environments. However, in its present implementation, there appear to be several free beam parameters whose effects on the observed field have so far been explored only by trial and error. Moreover, the application to reflection, refraction and diffraction phenomena has been based on *ad hoc* assumptions that introduce uncertainties, first, due to the assumed choice of reflection, transmission and diffraction coefficients and, second, due to the vague treatment of beam impact in diffraction regions, for example, near critical incidence or near structural discontinuities. It is

difficult to assess the quality of seismograms developed in this manner. It is proposed here to systematize these calculations by exploring the *proper* behaviour of the individual beam fields under various conditions alluded to above. This can be done efficiently by extending paraxial ray solutions for canonical trial problems to paraxial beam solutions via the complex source point substitution. Thus, the whole machinery of real ray theory, as incorporated into the geometrical theory of diffraction, can be utilized to provide the formulae needed for quantification of paraxial Gaussian beam phenomena, and for numerical studies of the influence of the various available beam parameters on the observed field. While the *ad hoc* approach employed so far for the generation of synthetic seismograms may indeed yield initial information in a convenient manner, the considerations above appear to be essential for any systematic attempt to improve the information contained in 'problematic' regions of the initial data, or to increase the confidence level in whatever initial discretization scheme one chooses to adopt.

Acknowledgment

This work was supported by the National Science Foundation under Grant No. EAR-8213147.

References

Aki, K. & Richards, P. G., 1980. *Quantitative Seismology: Theory and Methods*, W. H. Freeman, San Francisco.

Červený, V. I., Molotkov, I. A. & Pšenčík, I., 1977. *Ray Method in Seismology*, Karlova University, Praha.

Červený, V., Popov, M. M. & Pšenčík, I., 1982. Computation of wave fields in inhomogeneous media-Gaussian beam approach, *Geophys. J. R. astr. Soc.*, **70**, 109–128.

Červený, V. & Pšenčík, I., 1984. Gaussian beams in elastic 2-D laterally varying layered structures, *Geophys. J. R. astr. Soc.*, **78**, 65–91.

Chapman, C. H., 1978. A new method for computing synthetic seismograms, *Geophys. J. R. astr. Soc.*, **54**, 481–513.

Deschamps, G. A., 1971. Gaussian beams as a bundle of complex rays, *Electronics Lett.*, **7**, 684–685.

Einziger, P. D. & Felsen, L. B., 1982. Evanescent waves and complex rays, *IEEE Trans. Antennas Propag.*, **AP-30**, 4, 594–605.

Felsen, L. B., 1975. Complex rays, *Philips Res. Rep.*, **30**, 187–195, Special Issue in honour of C. J. Bouwkamp.

Felsen, L. B., 1976. Complex-source-point solutions of the field equations and their relation to the propagation and scattering of Gaussian beams, *Symp. Matemat.*, **XVIII**, 40–56, Istituto Nazionale di Alta Matematica, Academic Press, London.

Felsen, L. B., 1976. Evanescent waves, *J. opt. Soc. Am.*, **66**, no. 8, 751–760.

Felsen, L. B. & Marcuvitz, N., 1973. *Radiation and Scattering of Waves*, Prentice-Hall, New Jersey.

Ghione, G., Montrosset, I. & Felsen, L. B., 1984. Complex ray analysis of radiation from large apertures with tapered illumination, *IEEE Trans. Antennas Propag.*, in press.

Green, A. C., Bertoni, H. L. & Felsen, L. B., 1979. Properties of the shadow cast by a half-screen when illuminated by a Gaussian beam, *J. opt. Soc. Am.*, **69**, 11.

Heyman, E. & Felsen, L. B., 1983. Evanescent waves and complex rays for modal propagation in curved open waveguides, *SIAM J. appl. Math.*, **43**, 855–884.

Keller, J. B., 1965. Geometrical theory of diffraction, *J. opt. Soc. Am.*, **52**, 116–130.

Klem-Musatov, K. D. & Aisenberg, A. M., 1983. Ray method and the theory of edge waves, presented at the *Workshop on Seismic Waves in Laterally Inhomogeneous Media*, Liblice, June.

Nowack, R. & Aki, K., 1984. The 2-D Gaussian beam synthetic method: testing and application, *J. geophys. Res.*, in press.

Popov, M. M., 1982. A new method of computation of wave fields using Gaussian beams, *Wave Motion*, **4**, 85–97.

Ra, J. W., Bertoni, H. L. & Felsen, L. B., 1973. Reflection and transmission of beams at a dielectric interface, *SIAM J. Appl. Math.*, **24**, 396–412.

Shin, S. Y. & Felsen, L. B., 1977. Gaussian beam modes by multipoles with complex source points, *J. opt. Soc. Am.*, **67**, 5.